Simulation Using Realistic Spray Cooling for the Continuous Casting of Multi-component Steel

Houfa SHEN[†1)], *Richard A.Hardin*[1)], *Robert MacKenzie*[2)] *and C.Beckermann*[1)]

1) Department of Mechanical Engineering, The University of Iowa, Iowa City, IA 52242, USA

2) IPSCO Inc., Regina, Sask., S4P 3C7, Canada

[Manuscript received May 8, 2001, in revised form November 19, 2001]

A three-dimensional heat transfer model for continuous steel slab casting has been developed with realistic spray cooling patterns and a coupled microsegregation solidification model that calculates the solidification path for multi-component steels. Temperature and composition dependent properties are implemented in a database for 15 chemical species. Considerable effort is made to accurately model the spray cooling heat transfer. Each spray nozzle position and distribution is considered, including variations of the spray patterns with flow rate, and spray overlap. Nozzle type, layout, nozzle-to-slab distance, and spray span and flux are variable. Natural convection, thermal radiation and contact cooling of individual rolls are computed. The present model provides more comprehensive information and realistic slab surface temperatures than results from a model using the "averaged" treatment of boundary conditions. Cooling operating conditions and parameters of individual spray nozzles can be analyzed to optimize nozzle spray distribution, improve product quality, and troubleshoot issues such as nozzle clogging that may arise during production. One spray cooling correlation is used for the entire machine, achieving as good or better agreement with surface temperature measurements than was found previously for the model using an "averaged" treatment of boundary conditions and using three machine-segment-dependent correlations.

KEY WORDS: Steel, Continuous casting, Simulation

1. Introduction

The design of secondary spray cooling systems in continuous casting machines is mainly based on the requirements for maximum productivity, simplicity of operation, and ease of maintenance. A well-designed and operated spray cooling system contributes to a high quality of product without slab surface and inner defects. Heat transfer and cooling issues in continuous casting of steel slab have been investigated in numerous studies. Mathematical modeling of continuous casting varies greatly in model purpose, considerations, assumptions and approximations. Spray cooling and heat transfer have been investigated, and correlations of heat transfer coefficient with water flux and other variables have been reported[1~4]. In many models, the effects of spray cooling, natural convection, roll contact and thermal radiation are assumed to be constant or determined by an average heat transfer coefficient over segments in the machine[5,6]. The boundary conditions have been treated in some detail by modeling and measuring individual roll contact cooling[7]. The spray flux distributions on the slab surface and the related heat transfer properties have been experimentally determined[8]. Both linear latent heat release and prescribed non-linear solid fraction-temperature relations have been used to model latent heat evolution in solving the energy equation[5~7,9]. By coupling the energy equation to a back-diffusion microsegregation model[10], latent heat evolution (solid fraction-temperature relation, or solidification path) and solidus temperature are determined in the present model according to the local cooling history and composition[11,12].

In the past decades, many investigations have been focused on the influence of process parameters such as casting speed, steel grade and flow rate on the solidification length, shell thickness, and temperature profile using two-dimensional models[1~7,9,12,13]. Attention has recently been paid onto the effect of heat transfer through the strand surface on solidification defects such as cracking and macrosegregation[7,14]. Thermal stress and strain caused by inhomogeneous cooling and heat transfer induces the formation of cracks[1,15]. Obviously, a detailed consideration of cooling conditions based on realistic spray pattern modeling will be helpful for our understanding the heat transfer in continuous casting.

This paper describes the development of a three-dimensional heat transfer model of continuous casting using realistic spray cooling distributions, and it includes microsegregation to analyze the solidification behavior. Surface temperature predictions are shown to agree well with measurements, verifying the model and demonstrating that the model could be used for the optimization the nozzle layout and spray configuration for securing high quality of cast steel.

2. Experimental

Slab surface temperature measurements were made on a curved continuous slab caster with the radius of about 10 m by IPSCO Inc. These measurements were taken during production. Steel slabs of the same thickness but different section widths were cast. The solidifying steel shell was formed initially in a water-cooled copper mold and then continued forming in the roll segments where cooling spray was applied. Slabs were then cut off from the strand by a torch and transported away for further processing. Nozzles were arranged over roll gaps on the slab upward and downward facing surfaces. Nozzle types and placement were determined based on the casting conditions and slab width. Water flow rate in each cooling loop to a bank of nozzles was prescribed according to a casting speed dependent table that was designed to provide the required cooling for the product. Depending on slab width, the spray might extend beyond the slab edge, and depending on spray span and nozzle-to-nozzle distance, sprays might overlap. Figure 1 presents the relationship between the water pressure and flow rate for a certain nozzle type. Spray span on the slab surface was determined based on the water pressure and the nozzle-to-slab distance as shown in Fig.2.

A procedure was established at IPSCO Inc.[16] to measure the water flux distribution characteristics of the nozzles used on the machine. These characteristics were then built into the model based on the measurements provided by IPSCO Inc. In the nozzle flow measurements[16], an array of holes 25.4 mm in diameter was drilled in a plastic sheet, 2.44 m wide by 0.3 m high and 12.7 mm thick. The holes were arranged 5 rows high and 61 columns wide. The holes were spaced 38.1 mm apart in the width direction, and 59.7 mm apart in the height. A

† To whom correspondence should be addressed
E-mail: shen@tsinghua.edu.cn, Assoc. Prof., Ph.D.

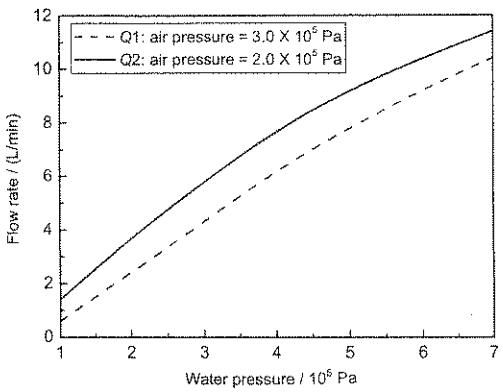

Fig.1 Relationship between water pressure and flow rate

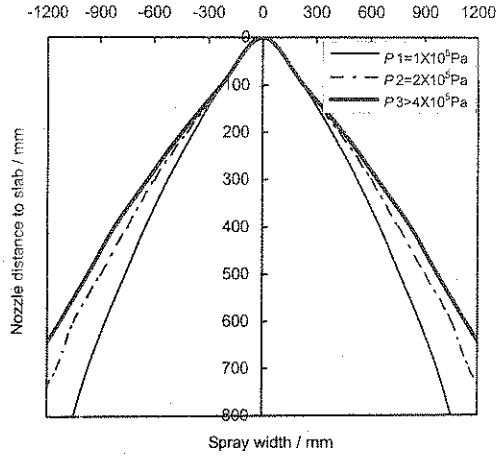

Fig.2 Spray width and distance from the tip of nozzle to slab surface at different water pressures

PVC tubing with outer diameter of 25.4 mm was glued into the holes in plastic sheet. The top row of tubing protruded 3.8 mm from the plastic sheet, and each subsequent row down protruded 1.3 mm more than the row above it. A shutter was installed in front of the array to precisely control the start and end of the flow. The shutter was rapidly opened at the start of a timed sequence so that all tubes were exposed to the spray for the same duration. An example measurement of the water flux determined by the aforementioned method is shown in Fig.3, with the nozzle distance to the plastic sheet d, the average water flow rate Q, and the responding nozzle type given on the legend. It was found that the water flux was unevenly distributed with a peak near the outer edge of the spray span. Spray flux distributions were obtained for a number of different flow rates. The measured flux distributions were stored and accessed by the simulation program pre-processor. Then depending on the water flow through each nozzle an accurate spray flux distribution for a given nozzle and flow rate was mapped to the surface of continuous casting model for use in determining the boundary conditions. The spray span and water flux distribution were adjusted in the model according to the casting speed, the spray intensity table used, and water flow characteristic of nozzles based on the measurements made by IPSCO Inc.

3. Model Description

Features of this model of continuous casting are three-dimensional geometry, temperature depended properties, and non-uniform mesh generation. Steady-state operation is assumed, and energy transport in the casting direction is advected by the casting speed only and conduction in this direction is neglected. The effects of convection in the liquid and solidifying mush are approximated using a thermal conductive enhancement factor β. The calculation domain is the whole slab region having coordinate axes x in thickness, y in width, and z in casting direction starting from the meniscus. The energy equilibrium equation describing the continuous casting process is

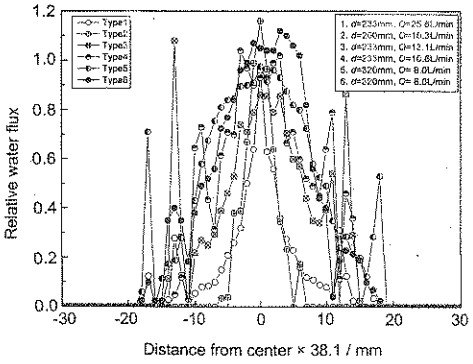

Fig.3 Relative nozzle spray water flux at a certain distance and a flow rate

$$V_{\text{cast}}\rho c_{\text{p}}\frac{\partial T}{\partial z}=\frac{\partial}{\partial x}\left(k_{\text{eff}}\frac{\partial T}{\partial x}\right)+\frac{\partial}{\partial y}\left(k_{\text{eff}}\frac{\partial T}{\partial y}\right)+S_{\text{l}} \quad (1)$$

where

$$\rho c_{\text{p}}=\varepsilon\rho_{\text{s}}c_{\text{p}_{\text{s}}}+(1-\varepsilon)\rho_{\text{l}}c_{\text{p}_{\text{l}}}$$

$$k_{\text{eff}}=[\varepsilon k_{\text{s}}+(1-\varepsilon)k_{\text{l}}][1+\beta(1-\varepsilon)^2]$$

$$S_{\text{l}}=V_{\text{cast}}\frac{\partial(\rho_{\text{s}}\varepsilon)}{\partial z}[L+(c_{\text{p}_{\text{l}}}-c_{\text{p}_{\text{s}}})(T-T_{\text{ref}})]$$

and V_{cast} is the casting speed in m/s, ρ density in kg/m^3, c_{p} is specific heat in J/kg·K, T temperature in K, k_{eff} thermal conductivity in W/m·K, S_l the energy source term in W/m^3, ε solid fraction, L latent heat in J/kg, T_{ref} reference value, and subscripts s and l denote solid and liquid respectively.

Temperature and composition dependent properties are implemented in a database of 15 chemical species. The liquidus slope of the i-th species element m_{l}^i, and its concentration in the liquid C_{l}^i determine the mush temperature T_{mush}.

$$T_{\text{mush}}=T_{\text{pure}}+\sum_i m_{\text{l}}^i C_{\text{l}}^i \quad (2)$$

Neglecting macrosegregation, the conservation of concentration of the i-th element during the solidification satisfies

$$C_0=\varepsilon C_{\text{s}}^i+(1-\varepsilon)C_{\text{l}}^i \quad (3)$$

The solid fraction-temperature relationship during solidification is a function of cooling rate and composition as determined through a microsegregation model[10] that is simultaneously solved with the energy equation

$$V_{\text{cast}}\frac{\partial}{\partial z}(\varepsilon C_{\text{s}}^i)=V_{\text{cast}}\kappa^i C_{\text{l}}^i\frac{\partial\varepsilon}{\partial z}+\frac{12D_{\text{s}}^i}{\lambda_2^2\varepsilon}(\kappa^i C_{\text{l}}^i-C_{\text{s}}^i) \quad (4)$$

where κ is the partition coefficient, D is the mass diffusion coefficient in m^2/s, and λ_2 is the secondary arm spacing in m.

Coupling Eqs.(1)~(4), four unknowns (T, C_{l}, C_{s} and ε) must be determined. The back-diffusion equation is solved by Newton-Raphson iterations[17]. Using a control volume based finite difference approach and ADI method[18], the energy equation is numerically solved with boundary conditions as described below.

In the primary cooling zone, mold heat flux is constant, prescribed by a function of dwell time in the mold. In the secondary cooling zone, the calculations account for cooling by spray convection, natural convection, thermal radiation, and thermal conduction to the containment rolls. Detailed boundary conditions are considered so that the individual roll contact regions, spray or non-spray regions are mapped onto the computational cells at the surface of the slab. Surface temperature measurements are compared with results of the heat transfer model to correlate surface boundary conditions and heat transfer coefficients. The resulting heat transfer coefficients are correlated with slab surface temperature, water spray flux and the temperature of the spray cooling water.

After parametric studies and calibration with the surface temperature measurements, the following correlation[15] of the heat transfer coefficient h_{spray} is used for spray cooling

$$h_{\text{spray}} = \frac{1570.0\ w^{0.55}[1 - 0.0075(T_{\text{spray}} - 273.15)]}{\alpha} \qquad (5)$$

where w is the spray cooling flux in L/m^2·s, T_{spray} is the temperature of the spray cooling water; and α is a machine dependent calibration factor. For the downward facing surface, the coefficient is modified to include the effect of plate orientation by multiplying the expressions for the upward facing surface by $(1-0.15\cos\theta)$, where θ is the slab surface angle from horizontal.

When the model determines that no spray is mapped to the surface of a computational volume, a standard correlation for natural convection is used. Thermal radiation is computed over the entire casting surface after the mold exits except at roll contact points. At the roll contacts, heat transfer coefficients are from measurements in the literatures [7,19]. An effective roll contact length of 10% of the roll diameter has been found to give good agreement with surface temperature oscillations previously observed due to roll contact cooling[7,19].

4. Calibration and Application

The equations described above are solved using a workstation running a 500 MHz 21264 Alpha processor. The model has a typical run-time of about 7 min for a 22×302×2002 grid (over 13 million control volumes). The user can perform simulations for a whole slab, or a half or quarter slab by applying symmetry. A spray flux distribution used by the model on the slab surface is shown in Fig.4(a); it has been made dimensionless by dividing its maximum value. The three-dimensional heat transfer and solidification model gives the temperature distribution as shown in Fig.4(b) for a slab 0.2032 m thick and 1.943 m wide. Casting speed is 0.8 m/min, pouring temperature is 1548°C, and the steel composition is 0.04 wt pct C, 0.30 wt pct Si, 1.64 wt pct Mn, 0.011 wt pct P, and 0.004 wt pct S. The calculated solidification length is 12.4 m (ε=1). The temperature varies in both width and casting direction. The correspondence between spray flux and surface temperature is apparent, *i.e.* the temperature is lower when intensive flux is sprayed on the surface. The temperature results calculated using "even" (or uniform spray distribution) and "uneven" (or nozzle mapped spray distribution) spray distributions with the same flow rate Q in each cooling loop, are shown in Fig.5. At the slab center, the temperatures are almost same for both cases until the slab is fully solidified. However, on the slab surface, the temperature oscillation is larger for uneven spray cooling not only because of roll contact cooling but also because of the larger spray flux variations. The further down the caster, the larger the difference in the two results. Examining the unbending region of the machine at about 17.6 m from meniscus, the realistic nozzle mapped spray results show a lower surface temperature by about 50°C in this region. In this case, the more realistic spray results would indicate a greater possibility of cracking than the uniform spray model for microalloyed steel grades having lower ductility strength below about 900°C.

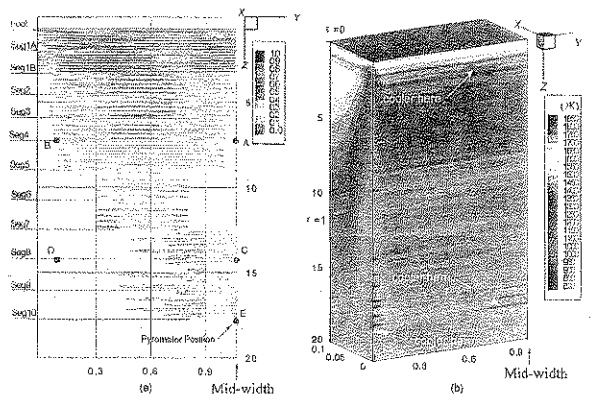

Fig.4 (a) Schematic of relative water flux on slab surface and (b) temperature distribution on the slab

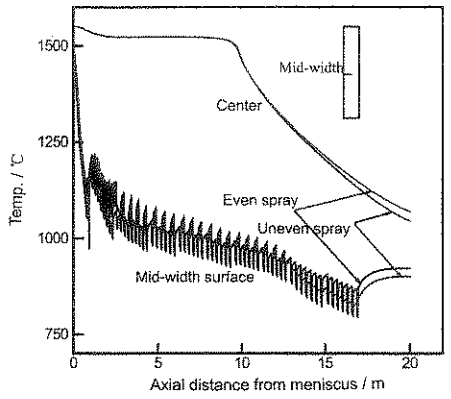

Fig.5 Temperature profiles at the center and mid-width of slab with even and uneven water flux in cooling loop

A series of surface temperature measurements from 17 casting sequences were made by IPSCO Inc. to calibrate the three-dimensional heat transfer model. The following casting parameters were varied in these sequences: slab width (1.23~1.94 m), concentration (0.034~0.346 wt pct C), and casting speed (0.8~1.06 m/min). Since the spray flux and flow rates varied with casting speed, the flows were varied according to the operating practice for the machine. The temperature was measured by IPSCO Inc. using seven pyrometers with uncertainties ranging from ±21.4 to ±29.1°C. Their accuracy was established from bias errors given in the manufacturer's data, and repeatability and reproducibility errors established from statistical analysis of the 17 casting sequences. The pyrometer positions in Fig.4(a) were as follows: "A" was located at the center of width between the fourth and fifth machine segments, two pyrometers were positioned at "B" between the fourth and fifth machine segments at both edges of the slab width (termed east and west edges), "C" was located at the center of the slab width between the eighth and ninth machine segments; two pyrometers were positioned at "D" near both edges between the eight and ninth machine segments; and "E" was located at the slab width center 18.45 m from the meniscus. The distances from the slab edge of test points "B" and "D" ranged from 25.4~127 mm. Example surface temperature measurements for five of the pyrometers are shown in Fig.6 for over 6 h of steady operation. After statistically analyzing the data, the average temperature and standard deviation were obtained. Figure 7 presents a comparison of the measured and predicted surface temperature obtained using the three-dimensional model for all pyrometers and casting sequences. Simulated temperatures and measure-

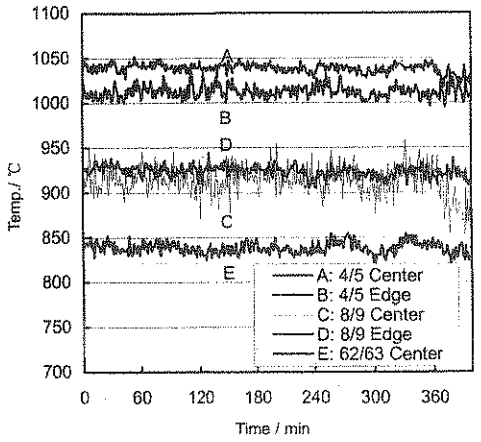

Fig.6 Surface temperature measurements at the points shown in Fig.4(a) with casting speed of 1.0 m/min, slab width of 1.23 m and carbon content of 0.065%

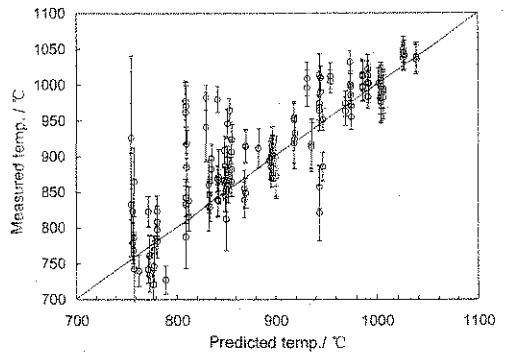

Fig.7 Comparison of predicted and measured surface temperatures for five pyrometer positions and 20 casting sequences

ments are shown to be in good agreement with an average error of 26°C. These results were obtained using a calibration factor α of 4 in the spray cooling correlation.

5. Conclusion

A three-dimensional heat transfer and solidification model for continuous casting of steel has been developed using realistic spray patterns and microsegregation calculations to accurately determine the solidification path. The model considers the spray cooling, natural convection, thermal radiation and roll contact heat transfer in the secondary cooling zone and gives more comprehensive information about the surface temperature variation than does a model using an averaged treatment of the boundary conditions. Nozzle layout, nozzle type, nozzle-to-slab distance, and each spray span and flux at different water pressures are variable in the model. This enables improved modeling, design and optimization for the spray cooling water flow distribution to better control continuous steel casting quality. Temperature and composition dependent properties are implemented in a database for 15 chemical species. Temperature and solid fraction in any sections of the slab along caster length, thickness and width can be calculated. Surface temperature profiles along the caster at any width or thickness position can be predicted. By using a machine dependent calibration factor α of about 4, predicted and measured slab surface temperatures show good agreement with an error of 26°C for a variety of casting conditions, alloys, widths, casting speed, and flow rate conditions.

Acknowledgement

The authors are grateful to IPSCO Inc. for supporting this research program and for providing surface temperature measurements, and measurements of the spray nozzle flow characteristics. Without the nozzle flow pattern measurements made by Dr. L.K.Chiang, this work would not have been possible.

REFERENCES

[1] J.K.Brimacombe, I.V.Samarasekera and J.E.Lait: *Continuous Casting* Vol.2, Heat Flow, Solidification, and Crack Formation, Book Crafter Inc., Chelsea, MI, 1984, 1-238.
[2] J.K.Brimacombe, P.K.Agarwal, S.Hibbins, B.Prabhaker and L.A.Baptista: *Continuous Casting,* eds. J.K.Brimacombe, I.V.Samarasekera and J.E.Lait, ISS-AIME, 1984, **2**, 109.
[3] B.G.Thomas: *Proc. 74th Steel Making Conference,* ed. The Iron and Steel Society, Warrendale, PA, 1991, **74**, 105.
[4] K.Sasaki, Y.Sugitani and M.Kawasaki: *Tetsu-to-Hagané*, 1979, **65**, 90.
[5] B.Lally, L.Biegler and H.Henein: *Metall. Trans. B*, 1990, **21B**, 761.
[6] S.Louhenkilpi, E.Laitinen and R.Nieminen: *Metall. Trans. B*, 1993, **24B**, 685.
[7] M.El-Bealy, N.Leskinen and H.Fredriksson: *Ironmaking and Steelmaking*, 1995, **22**, 246.
[8] Guanghua WEN, Jinghao CHI and Yunfei HUANG: *Research on Iron & Steel*, 1997, **98**, 3. (in Chinese)
[9] C.L.DeBellis and S.E.LeBeau: *National Heat Transfer Conf.*, ed. ASME, New York, NY, 1989, **113**, 105.
[10] C.Y.Wang and C.Beckermann: *Metall. Trans. A*, 1993, **24A**, 2787.
[11] R.A.Hardin, H.F.Shen and C.Beckermann: *Modeling of Casting,* Welding and Advanced Solidification Process IX, Aachen Germany, 2000, 729.
[12] R.A.Hardin and C.Beckermann: *National Heat Transfer Conf.*, ed. ASME, New York, NY, 1997, **9**, 9.
[13] S.K.Choudhary and D.Mazumdar: *ISIJ Int.*, 1994, **34**, 584.
[14] M.R.Aboutalebi, M.Hasan and R.I.L.Guthrie: *Metall. Mater. Trans. B*, 1995, **26B**, 731.
[15] T.Nozaki: *Trans. ISIJ*, 1978, **18**, 330.
[16] L.K.Chiang: *Internal Report on Secondary Spray Cooling System*, 1994, IPSCO Inc., Regina, Sask.
[17] M.C.Schneider and C.Beckermann: *Metall. Mater. Trans. A*, 1995, **26A**, 2373.
[18] S.V.Patankar: *Numerical Heat Transfer and Fluid Flow*, McGraw-Hill, New York, 1980, 1-197.
[19] R.York and K.H.Spitzer: *Solidification Processing 1997-Proc. 4th Decennial International Conference on Solidification Processing,* eds. J.Beech and H.Jones, University of Sheffield, 1997, 163.